

Cite this: DOI: 10.1039/c0xx00000x

www.rsc.org/softmatter

PAPER

# Adsorption of carboxylic modified latex particles at liquid interfaces studied by the gel trapping technique

Hamza Al-Shehri<sup>a</sup>, Tommy S. Horozov<sup>a</sup>, and Vesselin N. Paunov<sup>\*a</sup>*Received (in XXX, XXX) Xth XXXXXXXXXX 20XX, Accepted Xth XXXXXXXXXX 20XX*

DOI: 10.1039/b000000x

We have studied how carboxylic modified latex (CML) microparticles adsorb at liquid surfaces and the preferred type of emulsion they can stabilise depending on the particle size and the surface density of carboxylic groups. We measured the particle contact angle by using the gel trapping technique (GTT) for CML particles adsorbed at air-water and oil-water interfaces. Using this method we obtained scanning electron microscopy (SEM) micrographs of polydimethylsiloxane (PDMS) replicas of the liquid interface with the particles, where the PDMS replicates the non-polar phase and measured the particle contact angle. We discovered that the particle wettability correlates well with their surface density of the carboxylic groups but is not very sensitive on the presence of electrolyte in the aqueous phase and the value of the particle zeta potential. We demonstrated that CML microparticles of high surface density of COOH groups stabilise oil-in-water (O/W) emulsions while these with the lowest coverage with COOH groups favour the formation of water-in-oil (W/O) emulsions. We found that this corresponds to a change of the CML particle contact angle from lower than 90° to higher than 90° upon decrease of the surface density of COOH groups. The findings confirm that the surface density of polar groups has much bigger effect on the particle wettability and the preferred emulsion than the particle surface charge and zeta potential. Our results on the type of stabilised Pickering emulsion agree with other experimental studies with different particle materials. We propose an alternative explanation of the link between the particle contact angle and the type of stabilised Pickering emulsion.

## 1. Introduction

The wettability of the powder particles by liquids has attracted considerable interest during the last few decades due to its importance in formulation of pharmaceutical, cosmetic and food products, preparation of building materials and paints, waste water treatment, as well as in secondary oil recovery.<sup>1-4</sup> In all these cases, small solid particles adsorb or transfer through at the interface between a liquid phase and another fluid. The affinity of these particles to the adjacent fluid phases is characterised by the equilibrium three-phase contact angle,  $\theta$ , which is related to the surface energies of the liquid-fluid interface and the particle-fluid interface exposed to the two fluid phases. In many technological applications one of the fluid phases is water and the value of the particle three-phase contact angle reflects its hydrophilic ( $\theta < 90^\circ$ ) or hydrophobic ( $\theta > 90^\circ$ ) character and its wettability at the water-fluid interface. The functionalisation of the particle surface with terminal groups of different polarity or ionisation ability than the particle core material can change its wettability by the surrounding fluids and would favour lower or higher contact angles.<sup>3, 5</sup> Knowledge of particle wettability is required in order to understand their interactions and behaviour at liquid interfaces.<sup>5, 6</sup> For

example, it is possible to predict the type of Pickering emulsion that may occur when using solid particles as emulsifiers by measuring the particle contact angle.<sup>3, 6-9</sup> Particle contact angles, smaller than 90° indicate that they tend to stabilise oil-in-water emulsions while contact angles higher than 90° show that the solid particles are more likely to stabilise water-in-oil emulsions.<sup>6-8, 10-12</sup> Similar relationships exist between the particle three phase contact angle and the formation of particle stabilised foams and liquid marbles.<sup>13-16</sup>

Several crude and approximate methods for estimation of the wettability of powder particles by liquids are still in use in the industry. Washburn method<sup>17</sup> is designed to determine the particle contact angle from the capillary rise of liquid in a porous media produced by packed powder particles. However, the particle contact angles measured by the Washburn method can be affected by the porosity of the packed powder, the packing methodology and the particle swelling, which can yield different contact angles than those of the individual particles in uncompressed powders. Very similar issues exist in the compressed powder tablet method<sup>18, 19</sup> which relies on measuring the macroscopic contact angle of a liquid drop deposited on the powder tablet surface. Due

to surface roughness effects,<sup>20</sup> these methods cannot determine the contact angle of individual particles in the powder. In 2003, Paunov<sup>3</sup> proposed a conceptually different method that can measure the contact angles of individual microparticles and nanoparticles, known as the gel trapping technique (GTT) combined with scanning electron microscopy (SEM)<sup>3, 21, 22</sup> or atomic force microscopy (AFM).<sup>23</sup> The GTT<sup>3</sup> involves spreading of the studied solid particles dispersed in a spreading solvent (methanol, isopropanol) at the interface between an aqueous solution of a gelling agent and another immiscible fluid phase (oil or air). The adsorbed particles are then trapped at the liquid interface by gelling the aqueous phase and replacement of the top phase by curable silicone (PDMS) which after curing allows the particle monolayer to be peeled off from the liquid surface and imaged with a high resolution SEM or an AFM. The measurement of the particle protrusion from the PDMS surface allows the particle contact angle at the original liquid interface to be calculated.

Maestro *et al.*<sup>10</sup> and Isa *et al.*<sup>11</sup> pointed out that the spreading solvent may affect the properties of the particles and their contact angle. Maestro *et al.*<sup>10</sup> investigated the effect of the spreading solvent and determining the contact angle for different types of particles at the air-water and oil-water interfaces. They found that for different surface activities of methanol and isopropanol cannot change the surface tension when adding the same amount to the air-water or the oil-water interface.<sup>10</sup> Cayre and Paunov outlined that for very hydrophilic ( $\theta < 20^\circ$ ) or very hydrophobic particles ( $\theta > 160^\circ$ ), the GTT might have problems because of insufficient adhesion of the PDMS elastomer to the particles' or to the hydrogel after replacement of the PDMS with oil.<sup>21</sup> The GTT method has also been used to measure the contact angle of spherical and anisotropic particles,<sup>22</sup> food colloids<sup>9</sup> and porous particles, as well as microparticles functionalised with hydrophilic polymer brush layers.<sup>24</sup>

There are several alternative methods for measuring the contact angle of individual particles which should also be mentioned. A microparticle tensiometry method was designed by Butt *et al.*<sup>25, 26</sup> for determining the wettability of particles at air-water surface by measuring the deflection of an AFM cantilever with a fixed colloidal particle which is attached to the air-water interface. A force curve is observed before, after attachment and detachment of the colloidal probe to and from air-water surface. This method can be used for measuring the absorption energy of particles from the air-water surface and can determine both advancing and receding contact angles, but is only applicable to micron-size particles. Recently, Horozov *et al.* developed the film-calliper method (FCM) for measuring the contact angle of micrometre and sub-micrometre particles at the air-water interface.<sup>6</sup> This method requires that particles are bridging both surfaces of an aqueous film. The particles are injected and spread at a horizontal air-water surface to form a diluted particle monolayer which is then picked up by vertical frame where the particles get trapped in a liquid film. By observing the aqueous film with a horizontal microscope, the bridging particles position can be localised alongside with the Newton interference fringes of liquid meniscus. The reconstruction of the meniscus profile together with the bridging particle position makes it possible to estimate the contact angles of microparticles

in real time. The FCM works for hydrophilic particles that bridge the surfaces of the aqueous film and cannot be applied for hydrophobic particles. Recent studies of the contact angles of latex particles with grafted hydrophilic polymer brushes indicated that the FCM gives the receding contact angle.<sup>24</sup> Very recently, Isa *et al.* developed a variation of the GTT using freeze-fracture, shadow-casting (FreSCa) congregated with cryo-SEM which was applied to hydrophobic and hydrophilic spherical colloidal particles of different sizes and surface chemistry trapped at the interface between oil-water. This method uses similar approach as the gel trapping technique to trap the particles at the liquid interface but by freezing the water phase, thus avoiding the gelling and PDMS micro-casting steps. The particles are shadow casted by metallic layer deposition at different angles which allows to compute the protrusion of the particle interface above the ice surface and calculate the particle contact angle if the particles diameter is known.<sup>11</sup>

Particle contact angles are important to predict the type of preferred emulsion when colloid particles are used as emulsifiers. The stability and type of emulsions stabilised by pre-hydrophobised silica nanoparticles<sup>27</sup> were investigated for particles of different percentage of remaining silanol groups ( $-\text{SiOH}$ ) on the particle surface. It has been confirmed that the emulsion type formed depends on the particle wettability. Hydrophilic particles stabilised oil-in-water emulsion while hydrophobic ones formed water-in-oil emulsions.<sup>27</sup> Similar relations between the particle wettability and the formation of stable foams and liquid marbles have been discussed.<sup>15</sup>

In this paper, we have used the gel trapping technique (GTT) to study how latex particles with different number of carboxylic group per unit surface area adsorb at the air-water and the oil-water interface and how this affects the particle wettability at both liquid interfaces. We also investigated the effect of the particle injection at the liquid interface thorough both the aqueous and the non-polar phase on the measured particle contact angle with the GTT. Furthermore, we also looked at the type and stability of emulsions stabilised by latex particles with various surface densities of carboxylic groups and correlated the results with the measured particle contact angle. The results of this study are important for better understanding of the link between the surface functionality of the emulsifier solid particles and preferred type of emulsion.

## 2. Experimental

In this section we describe the materials and the methods used for measuring the contact angle of carboxylic modified latex microparticles by the GTT, and the variation of the method of injecting the particles to the liquid interfaces as well as the preparation of emulsions stabilised by CML particles.

### 2.1 Materials

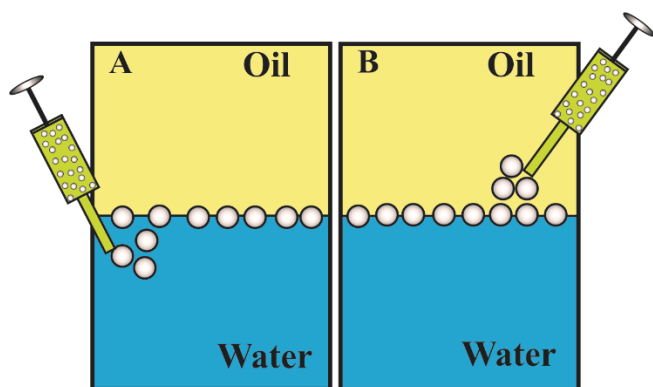
We used CML particle samples of varying diameters: 0.90  $\mu\text{m}$ , 1.2  $\mu\text{m}$ , 2  $\mu\text{m}$ , and 3  $\mu\text{m}$ , respectively, which were purchased from Invitrogen as aqueous suspensions. These carboxylic modified latex particles have negative surface charge in aqueous media due to the dissociation of the carboxylic groups on their surfaces which are functionalised with different amounts of an anionic polymer.

Cite this: DOI: 10.1039/c0xx00000x

www.rsc.org/softmatter

## PAPER

The carboxylic groups of the CML particle surface are fully ionized above pH 10. Hexadecane and dodecane (Reagent Plus 99%, from Sigma) were purified by passing three times through chromatographic alumina. Activated aluminium oxide (STD 5 Grade, from Merck) was used to remove any polar impurities from these oils. Gellan gum (Kelcogel®), was a gift from CPKelco (USA). Sylgard 184 curable elastomer (polydimethylsiloxane, PDMS) was obtained from Dow Corning. Strata C<sub>18</sub>-silica functionalised chromatographic column (Gigatube, 60 mL, from 10 Phenomenex) was used to remove any hydrophobic or surface active impurities from aqueous gellan gum solutions before the GTT experiment. Ethylenediaminetetraacetic acid disodium salt (EDTA, 99.6 %) and sodium hydroxide (NaOH, 99.6%) were purchased from Sigma. Sodium chloride (NaCl, 99.5%) was 15 supplied by BDH. The aqueous solutions used in these experiments were prepared with deionized water (resistance > 18.2 Ω) from a Millipore Milli-Q Plus water purification system.



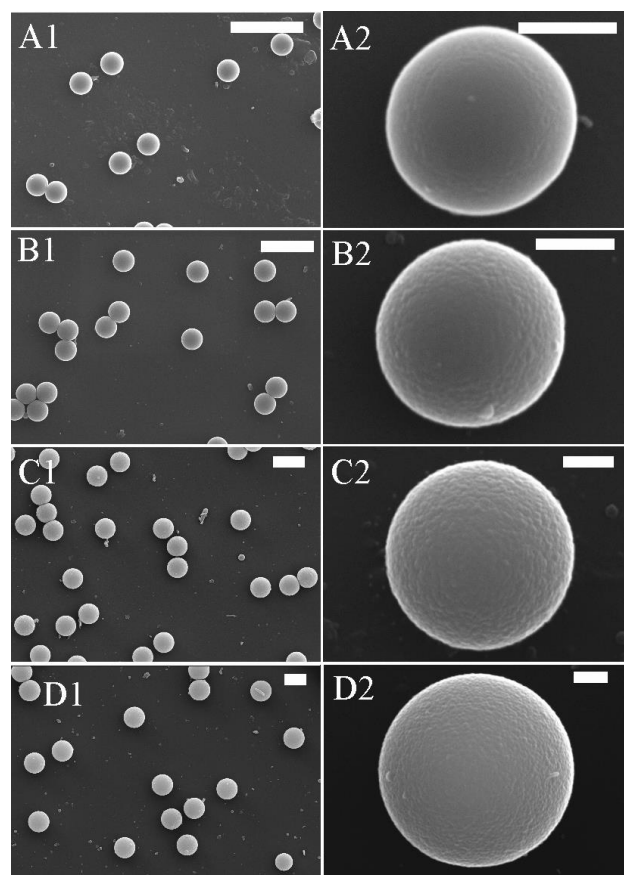
20 **Figure 1.** Schematics of injection of the particle spreading suspension close to the interface between the non-polar phase (oil or air) and the gellan solution. In our experiment we explored injecting of the particles suspension through (A) the water phase and (B) the oil (or air) phase.

## 2.2 Methods

### 2.2.1 Replication of the colloid particle monolayers at liquid surfaces by using the GTT

**Preparation and purification of the gellan solution.** The gellan gum used in the gel trapping technique was purified to achieve low 30 surface activity at the air-water or the oil-water surface. 3.0 g gellan gum powder was dispersed in 600 mL Milli-Q water at 95 °C in a water bath for 30 minutes to hydrate the polymer. The obtained 0.5 wt% gellan solution was brought to 50 °C and passed twice through a pre-activated C<sub>18</sub>-silica chromatographic column 35 connected to a vacuum filtration set. The latter was pre-activated using acetonitrile-water mixture (80:20) and flushed several times with hot Milli-Q water before the hot gellan solution was passed through it. The C<sub>18</sub>-silica column was heated from outside during the filtration of the hot gellan solution to prevent its gelation on the 40 inside the column. Finally, after the purification step, the gellan

solution was concentrated by evaporation at 90 °C from 0.5 wt% in (600 mL) to approximately 2 wt% (150 mL).<sup>3, 21</sup> The final concentration of gellan was confirmed gravimetrically by complete evaporating an aliquot from the solution. The 45 concentrated solution was kept at 60 °C in a sealed flask till its use in the GTT experiment.



50 **Figure 2.** Scanning electron micrographs of the CML particles of various diameters studied in this paper: (A1, A2) 0.9 μm, (B1, B2) 1.2 μm, (C1, C2) 2 μm, and (D1, D2) 3 μm. High resolution SEM images (A2-D2) showing the local surface morphology for the CML particles. The scale bars are 3 μm for images (A1-D1) and 500 nm for images (A2-D2).

**Spreading the CML particles at the air-water and the oil-water interface.** The aqueous suspensions of CML particles were mixed with methanol (50:50 by mass), which was used as a spreading solvent. The oils were pre-warmed up to 50°C to match the temperature of the purified gellan solution. 3 mL of the hot 2 wt% gellan solution was poured into a preheated plastic Petri dish (50-55 °C) of diameter 40 mm and the same amount of the preheated 60 oil phase was carefully introduced on top of the gellan solution. We explored the importance of the phase from which we spread the particles at the interface on the particle contact angle. A small sample (typically 20 μL) of the CML particle suspension in 65 water/methanol solution was spread at the oil-water interface using

two different approaches by injecting it through the oil phase (i) or through the water phase (ii) close to the liquid interface, as illustrated the Figure 1. The gellan phase with the adsorbed particles was kept at 25 °C for 30 minutes until gelling, then the oil phase was decanted off and its residue was carefully removed from edge of the Petri dish by using a string of tissue paper. PDMS was mixed in a ratio of (10:1) with its curing agent and centrifuged to remove any air bubbles forming in the PDMS during mixing. The PDMS was carefully layered over the gelled aqueous phase with the particle monolayer to avoid trapping of air bubbles and was cured for 48 hours at 25 °C in an incubator (Stuart SI500). After peeling off the solidified PDMS layer with the particles, the samples were incubated in hot aqueous solutions of 20 mM of EDTA disodium salt, 20 mM sodium hydroxide, and Milli-Q water were used for 20 min respectively, to wash off the gellan residues from the PDMS surface. We used this procedure for CML particles adsorbed at both the dodecane-water and hexadecane-water interface. In the case of CML particles at the air-water interface the procedure was very similar, however, the Petri dish was sealed during the gelation process to avoid evaporation of water and development of cracks at the hydrogel-air interface. In this case the particle monolayer was micro-casted with PDMS directly from the surface of the set gellan solution.

**2.2.1 Effect of the salt concentration in the aqueous phase on the particle contact angle at the air-water and the oil-water interface.**

We investigated the effect of addition of NaCl to the aqueous phase on the three-phase contact angle of 3 μm CML particles at the liquid interface. Solid NaCl was added directly to the purified gellan solution to adjust the salt concentration to 1 mM of NaCl. The aqueous suspension of the 3 μm CML particles was mixed with methanol in 50:50 by mass then spread at the liquid interface. The oil phases used in this experiment were dodecane, hexadecane, and tricaprylin. Sample preparation was carried out as described in the previous section.

**2.2.2 Preparation and characterising of CML particle stabilised emulsions.**

2 mL of 5 wt% aqueous suspension of CML particles in 1mM NaCl was stained by 10<sup>-5</sup> M fluorescein sodium salt. Then 2 mL of dodecane was added and mixed by vigorous hand shaking for 30 seconds at 25 °C. The emulsions samples were imaged

immediately after preparation and the type of the droplet phase was determined using fluorescence microscopy (Olympus BX-51 microscope fitted with FITC filter set).

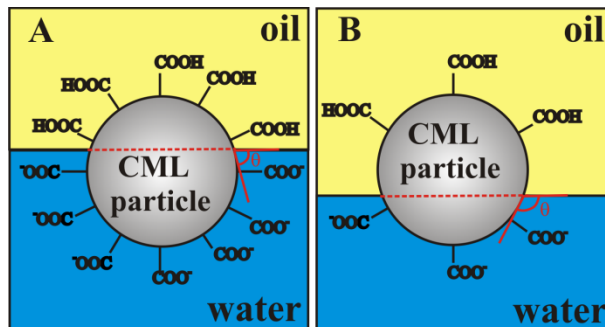


**Figure 3.** Schematic representation of the effect of carboxylic (-COOH) surface groups on the particles adsorption and three-phase contact angle at oil-water interface: (A) high surface density of carboxylic groups on the particle surface makes them hydrophilic ( $\theta < 90^\circ$ ), while (B) low surface density of carboxylic groups on the latex particle surface turns them hydrophobic ( $\theta > 90^\circ$ ).

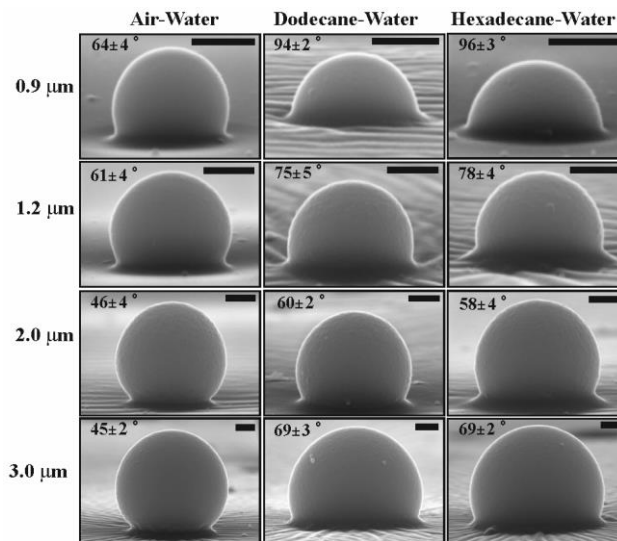


**Figure 4.** SEM micrographs of CML particles of different diameter and their contact angles at the air-water, dodecane-water and hexadecane-water interfaces. For the samples on these SEM mages the particles dispersion in the spreading solvent was injected at the liquid interface through the water phase. The detector tilt angle used for imaging the particles was 85°. The scale bar is 500 nm on all images.

Table 1. Data for the CML particles of different size and the particle three-phase contact angle measured at the air-water and oil-water interfaces after a particle injection through the water or the oil phase. The contact angle values reported in this paper are an average of at least 10 measurements done on different particles from several SEM images over at least two repeated samples. The error bars represent the standard deviation of the contact angle data.

Particle diameter <sup>a</sup> / μm	Number of COOH groups per particle <sup>a</sup>	Area per surface carboxyl group / nm <sup>2</sup>	air-water / θ°		dodecane-water / θ°		hexadecane-water / θ°	
			injection through air	injection through water	injection through dodecane	injection through water	injection through hexadecane	injection through water
0.9	5.5 × 10 <sup>6</sup>	4.6	63 ± 3	64 ± 4	96 ± 3	94 ± 2	97 ± 3	96 ± 3
1.2	3.5 × 10 <sup>7</sup>	1.3	64 ± 3	61 ± 4	67 ± 7	75 ± 5	82 ± 5	78 ± 4
2.0	4.1 × 10 <sup>8</sup>	0.3	50 ± 2	46 ± 4	61 ± 5	60 ± 2	60 ± 1	58 ± 4
3.0	3.0 × 10 <sup>8</sup>	0.9	47 ± 2	45 ± 2	71 ± 3	69 ± 3	69 ± 3	69 ± 2

<sup>a</sup> Provided by the manufacturer

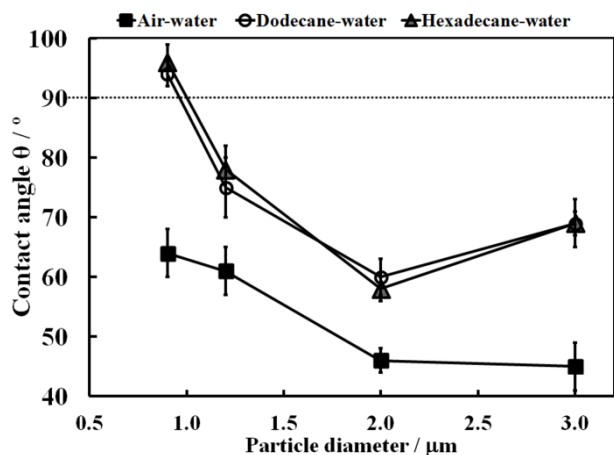


**Figure 5.** Three-phase contact angles of CML particles at the air-water, dodecane-water, and hexadecane-water interfaces vs. the particle diameter. Particle contact angles above  $90^\circ$  should favour the formation of water-in-oil emulsions. The lines between the data points are only guides to the eye.

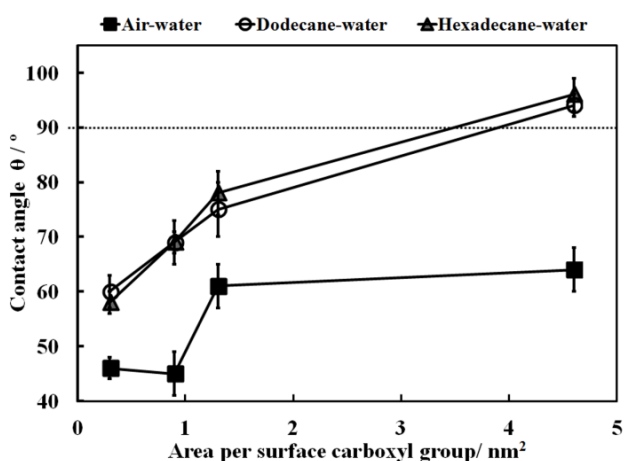


**Figure 6.** CML particle three-phase contact angle as a function of the area per carboxylic group on the particle surface. Large area per  $-\text{COOH}$  group corresponds to hydrophobic particles, while lower areas per  $-\text{COOH}$  group correspond to hydrophilic particles. The lines between the data points are only guides to the eye.

### 2.3 Contact angle of CML particles adsorbed at a liquid interface

The three-phase contact angles of the CML particle were determined from the SEM micrographs of the PDMS micro-casts of the liquid interface using the flowing analysis:

(i) If the particles contact line diameter was below the particle equatorial diameter (hydrophilic particles,  $\theta < 90^\circ$ ), the contact angle  $\theta$  was determined from the relationship:

$$\sin \theta = d_c / D. \quad (1)$$

Here  $D$  is the particle equatorial diameter;  $d_c$  is the particle contact line diameter.

(ii) For hydrophobic particles,  $\theta > 90^\circ$ , whose contact line is above the particles equatorial diameter, the contact angle was calculated by:

$$\sin(\pi - \theta) = d_c / D. \quad (2)$$

## 3. Results and Discussion

### 3.1 Wettability of CML particles at liquid surfaces

The morphology of the CML particles of different size and  $\text{COOH}$ -group density was studied by SEM. Figure 2 shows SEM micrographs of the used latex particles as provided by the manufacturer. Note that the  $0.9 \mu\text{m}$  CML particles surface appear significantly smoother than the CML particles of higher size.

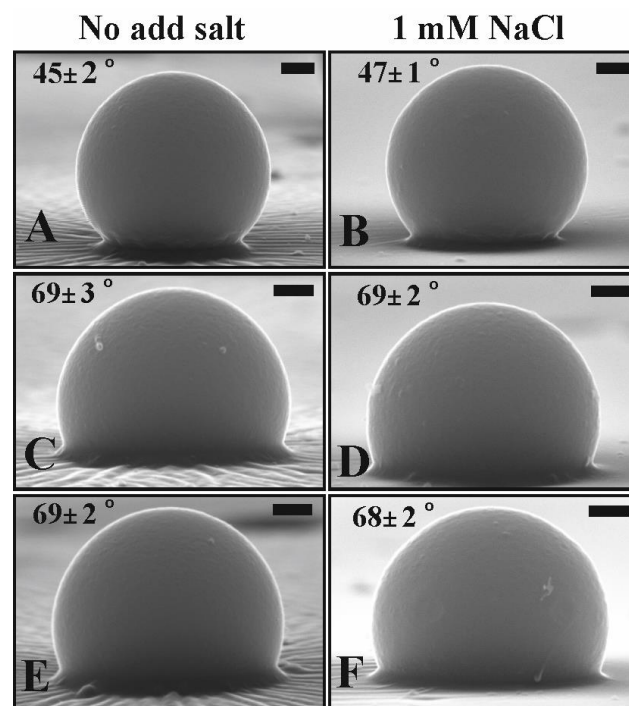


**Figure 7.** SEM images of  $3 \mu\text{m}$  CML particles templated with PDMS at different liquid interfaces where the particles are injected through the water phase. The contact angle does not change upon adding of known amount of  $\text{NaCl}$  ( $1 \text{ mM}$ ) to the aqueous phase (A and B). Typical SEM images of the CML particles at the air-water surface; (C and D) at the dodecane-water interface and (E and F) at the hexadecane-water interface. The scale bar is  $500 \text{ nm}$  on all images.

Figure 4 shows SEM micrographs of CML particles gel-trapped and micro-casted with PDMS at the air-water surface, the dodecane-water and hexadecane-water interfaces (see Table 1). The visible part of particle surfaces on the PDMS has been immersed in the water phase while the particle surface immersed by the PDMS has been originally in the air or oil phase. We calculated the particle contact angle by using Eq 1 or Eq 2 after measuring the contact line diameter of the individual particles from the SEM images,  $d_c$ , and fitting a circular profile on the particles to determine their equatorial diameter,  $D$ . Note that the CML particle contact angles are affected by the area per carboxylic group on the particle surface. Smaller surface density of carboxylic groups on the particles surface corresponds to higher contact angle. CML particles of diameter  $0.9 \mu\text{m}$  have the highest three-phase contact angle because the lowest surface density of COOH groups. These particles are hydrophobic ( $\theta \sim 96^\circ$ ) at the oil-water interface. We envisage that at low surface density of carboxylic groups, the two fluid phases have higher contact area with the bare polystyrene surface which has high contact angle at the oil-water interface ( $\theta > 120^\circ$ ).<sup>3</sup> The CML particles of diameter  $2 \mu\text{m}$  have the highest surface density of COOH groups which is reflected by their contact angle ( $\theta \sim 60^\circ$ ) at the oil-water interface. We note that the CML particle contact angle at air-water surface follow a similar trend with the area per carboxylic group as shown on Figure 6.

The calculations are done based on the parameters of our  $1.2 \mu\text{m}$  CML particles. The value of the zeta potential is used here as proxy for the respective surface electric potential. The particle surface charge density is estimated from the value of the zeta potential  $-36 \text{ mV}$  of the particle at pH 5 and salt concentration  $1 \text{ mM}$  (see Figure 8). The zeta potential of the air-water interface is assumed  $-40 \text{ mV}$ . The electric double layers free energy is calculated from Eq 4 and the particle contact angle from Eq 6. Note that the effect is very small – the change of  $\theta$  is within  $1^\circ$  over the range of salt concentrations.

We found that the particle contact angle measurements at the oil-water interface for CML particles injected through the aqueous phase give very similar results to these injected through the oil phase. One possible explanation is that the particles entry barrier at the liquid interface is overcome by the spreading solvent which drags the particles to the interface without significant difference with respect to the liquid phase in which the particles suspension is introduced in the system. Figure 5 represent how the particle contact angle depends on the particles diameter. However, the dependence is not at constant area per carboxylic group and reflects the variation of the polarity of the particle surface for the set of particles of varying size which have different number of carboxylic groups per unit area. The CML particle contact angle decreases with increasing of the particles size as this corresponds to higher surface density of carboxylic groups on the particle surface (Figure 6).

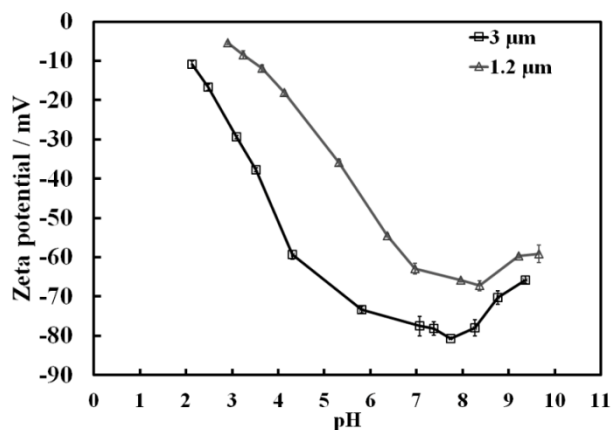


Figure 8. Zeta potential of the  $1.2 \mu\text{m}$  and  $3 \mu\text{m}$  CML particles as a function of pH at  $1 \text{ mM}$  NaCl in the aqueous solution. The zeta potential gradually changes with the pH. The lines between the data points are only guides to the eye.

### 3.2 Effect of the salt concentration on the contact angle of CML particles at liquid surfaces

We compared the contact angles of CML particles at the air-water and oil-water interfaces for the cases with and without addition of NaCl. The salt was added to the purified gellan solution at a concentration of  $1 \text{ mM}$  NaCl in  $2 \text{ wt\%}$  gellan. The results, which are represented in Figure 7 show that the addition of salt does not affect the contact angle. We did not test higher concentration of salt as high ionic strength solution may interfere with the ability of gellan to gel and form strong hydrogels which may compromise the contact angle measurements with the GTT. Note that the three-phase contact angle of  $3 \mu\text{m}$  CML particles at both the air-water and the oil-water interface does not change significantly upon the addition of salt to the aqueous phase. We estimated the effect of the electrolyte concentration on the Gibbs free energy  $\Delta G_{el}$  of the electric double layers at the particle-water interface and the air-water interface in an attempt to evaluate its influence on the particle contact angle. Neglecting the particle surface curvature effects for the sake of simplicity, we used the relation between the surface charge density  $\sigma_0$  and the particle surface potential<sup>28</sup>

$$\sigma_0 = \frac{2kT\epsilon\epsilon_0\kappa}{Ze} \sinh\left(\frac{\psi_0 Ze}{2kT}\right) \quad (3)$$

which allowed us to calculate  $\Delta G_{el}$  from the equation<sup>28</sup>

$$\Delta G_{el}(\psi_0) = -\left(\frac{2kT}{Ze}\right)^2 \kappa\epsilon\epsilon_0 \left[ \cosh\left(\frac{\psi_0 Ze}{2kT}\right) - 1 \right] \quad (4)$$

Here  $e$  is the electronic charge,  $N_A$  is the Avogadro's number,  $\epsilon_0$  is the vacuum permittivity,  $\epsilon$  is the dielectric constants of water;  $T$  is the absolute temperature, and  $k$  is the Boltzmann constant,  $Z$  is the valency of the electrolyte ( $Z:Z$ ) and  $\psi_0$  is the surface electric potential. In Eq 3 and Eq 4,  $\kappa$  is the Debye screening parameter which is calculated from the formula

$$\kappa = \sqrt{\frac{2000 Z^2 e^2 N_A^2 C_{el}}{\epsilon\epsilon_0 kT}} \quad (5)$$

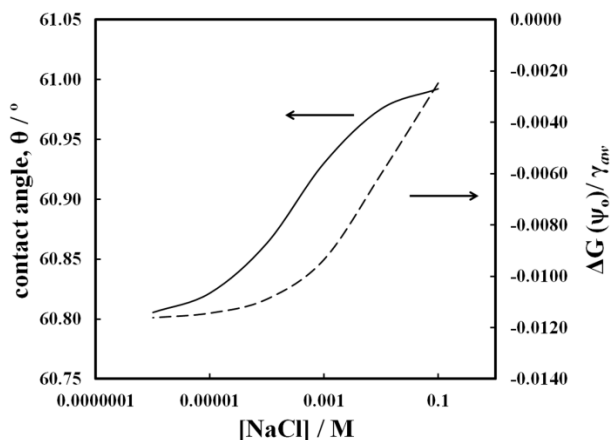


Figure 9. The estimated effect of the salt concentration on the CML particle contact angle based on the change of the electric double layer free energy.

Cite this: DOI: 10.1039/c0xx00000x

www.rsc.org/softmatter

## PAPER

where  $C_{el}$  is the electrolyte concentration. For these calculations we assume the air-water surface potential,  $\psi_{aw}$ , to be -40 mV. The CML particle surface potential is  $\psi_{pw} = -36$  mV which is approximated with its zeta potential in 1 mM NaCl at pH 5. If we assume that the particle contact angle corresponding to non-dissociated COOH groups is  $\theta_0$ , we estimate the effect of the electrolyte concentration on the particle contact angle from the expression<sup>29</sup>

$$\cos \theta = \frac{\cos \theta_0 - \Delta G_{el}(\psi_{pw})/\gamma_{aw}}{1 + \Delta G_{el}(\psi_{aw})/\gamma_{aw}} \quad (6)$$

Here  $\gamma_{aw}$  is the air-water surface tension,  $\Delta G_{el}(\psi_{aw})$  and  $\Delta G_{el}(\psi_{pw})$  are the surface free energy of formation of the electric double layers at the particle-water surface and air-water surface, having surface potential  $\psi_{aw} = -40$  mV and  $\psi_{pw} = -36$  mV at 1 mM NaCl. We calculated the three-phase contact angle vs. the salt concentration by using Eq 6 and assuming constant surface charge density for both the air-water and the particle-water interface. The calculation done here assumes constant surface charge at the air-water and the particle-water interface as the electrolyte concentration is varied. Our measurements showed that the 2% gellan solution has a pH 5. The respective values of  $\sigma_{aw}$  and  $\sigma_{pw}$  are calculated once from Eq 3 for the quoted values of the surface potentials 1 mM NaCl and pH 5 (see Figure 8). Then, at constant surface charge densities, we varied the salt concentration and recalculated the surface potentials from Eq 3 and the corresponding values of  $\Delta G_{el}(\psi_{aw})$  and  $\Delta G_{el}(\psi_{pw})$  from Eq 4 and the contact angle from Eq 6.

Figure 9 shows the calculated effect of the salt concentration on the particle contact angle at the air-water surface. However, as the graph shows the change of the microparticle contact angle for a wide variation of the salt concentration is very small, i.e. within 1°. Similar results are obtained upon variation of the particle surface charge density at fixed value of the surface potential. The particle surface curvature effect on the electric double layer surface energy is important only when the particle radius of curvature becomes comparable with the Debye screening length, as discussed in Ref.<sup>29</sup> For 1 mM NaCl solution the Debye screening length is two orders of magnitude smaller than the size of the microparticles used in this study. This is satisfied even for microparticles in milliQ water (typically of pH 5.5). For this reason, neglecting of the surface curvature effects is justified. Nevertheless, even with neglecting of the curvature effects, the overall contribution of the electric double layers to the variation of the particle contact angle was found to be very small as shown on Figure 9. Note that the particles have very different surface group densities and all of them show very small changes in the particle contact angle as the salt concentration increase to 1 mM. Hence the change of the particle contact angle measured experimentally cannot be explained solely due to changes of the free surface

energy of the electric double layer of the particles and the air-water surface as it is too small for particles of this size.<sup>29</sup> Although upon changing pH and salt concentration the COOH groups on the particle surface can dissociate to produce high surface charge density and corresponding surface potential, as illustrated in Figure 10 with the measured particle zeta potential versus the pH, the value of the contact angle seems to be determined by the surface density of the COOH group rather than their degree of ionisation. In addition to this argument, at the pH of the aqueous phase with the gellan in the GTT experiment the pH is around 5.5 where a high percentage of COOH groups on the CML particle surface are not dissociated. Hence one can correlate the COOH group surface density with the particle contact angle at the liquid interface. The same arguments hold for particles at the oil-water interface where similar analysis can be made that the effect of the polar carboxylic group present on the surface is the main factor determining the change of the particle contact angle.

### 3.3 Emulsions stabilised by CML particles

Using dodecane as an oil, CML particles (5 wt%) as sole emulsifier and 1 mM NaCl aqueous solution stained with fluorescent dye solution, we produced emulsion for all particle sizes used in this study (Fig. 10). Oil-in-water emulsions were obtained for CML particles of diameters 1.2  $\mu\text{m}$ , 2  $\mu\text{m}$ , and 3  $\mu\text{m}$  which, according to our GTT contact angle data are hydrophilic particles as their contact angle are lower than 90°. However, for the 0.9  $\mu\text{m}$  CML particles, whose contact angle at the decane-water interface is above 90°, water-in-oil emulsion was obtained. The general result from this study is that the solid particles surfaces are more exposed to the phase outside the droplets in the preferred type of a Pickering emulsion, as also shown by others.<sup>6-8, 10-12</sup> However, the physical reasons for this conclusion are barely discussed in the literature. The thermodynamic aspects of this result are considered in the recently published work by Kralchevsky *et al.*<sup>30</sup> Here we present an alternative view which is based on the fact that during the emulsion preparation (e.g. at 50:50 oil:water), both W/O and O/W emulsion drops coated with solid particles are formed simultaneously and undergo coalescence. It is very likely that their liquid interfaces are not closely packed with solid particles during this process as the emulsion is homogenised and the droplets come in contact with each other. Therefore the bridging effect of the solid particles in the liquid films formed between the emulsion drops determines which type of emulsions survives and leads to the preferred emulsion type. Hydrophobic particles can form stable oil film by bridging two water drops in oil but cannot form stable aqueous film by bridging two oil drops in water. Since the opposite is true for hydrophilic particles, this could explain the final outcome that hydrophobic particles stabilise W/O Pickering emulsion while hydrophilic particles stabilise O/W Pickering emulsions.

Cite this: DOI: 10.1039/c0xx00000x

www.rsc.org/softmatter

## PAPER

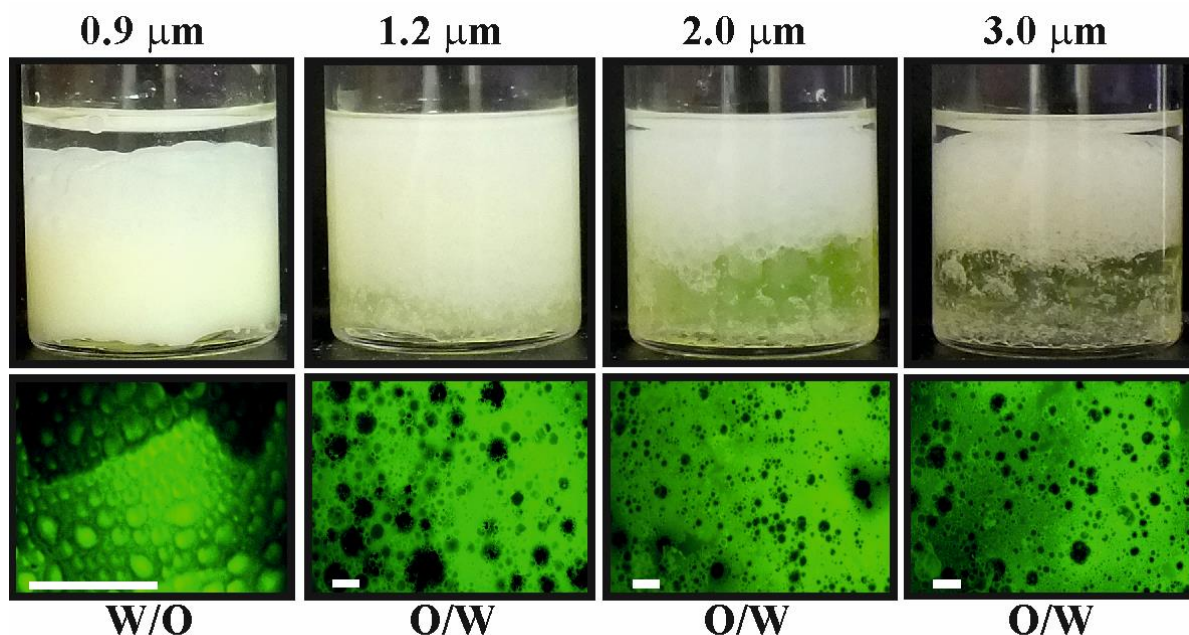


**Figure 10.** Optical photographs of emulsion made from 50:50 dodecane:water stabilised by 5 wt% CML particles in 1mM NaCl immediately after emulsification. The emulsification was done by using the hand-shaking method. Fluorescence microscope images of these particle stabilised emulsions where the aqueous phase has been doped with fluorescein. The type of the emulsion changed from (W/O) water-in-oil emulsion to oil-in-water (O/W) emulsions not due to different size of the particles but due to the decreasing area per COOH group on the particle surface which switches the particles from hydrophobic to hydrophilic. The scale bar is 200  $\mu\text{m}$  on all images.

#### 4. Conclusions

In this work we used the gel trapping technique (GTT) to study the three-phase contact angle of CML particles at the air-water and the oil-water interface for particle of varying size. We found that although the particle contact angle varies with the particle size, it turns out that the variation is due to the different surface density of carboxylic groups on the surfaces of CML particles. We also estimated the effect of the COOH groups' ionisation at the particle surface and the free energy of the electric double layer on the particle contact angle but it proved be too small to explain the variation in the particle contact angle. We also tested the role of the liquid phase from which the particles are injected at the liquid interface in the GTT experiment. The effect of the CML particles initial phase does not change the particle contact angle significantly within the experimental error. We also investigated both experimentally and theoretically the effect of the presence of salt in the aqueous phase on the particle contact angle and found that it is negligible at least for moderate salt concentrations. The main conclusion is that the CML particle contact angles are mostly determined by the density of carboxylic group on the particle

surface rather than by their ionisation at the particle surface. We also found that the CML particles with low density of COOH groups have contact angle higher than  $90^\circ$  at oil-water interface and prefer to stabilise the water-in-oil emulsions. The CML particles of contact angle lower than  $90^\circ$  had much higher surface density of COOH-groups and stabilise oil-in-water emulsion.

#### Acknowledgment

H. A. thanks the Ministry of Higher Education of the Kingdom of Saudi Arabia for the funding of his PhD studentship. We thank Mr Tony Sinclair for the sample preparation for SEM imaging.

<sup>a</sup> University of Hull, Cottingham Road, Hull HU6 7RX, United Kingdom  
Fax: +441482466410; Tel: +441482465660; E-mail:

V.N.Paunov@hull.ac.uk

#### References

1. J. T. Davies and E. K. Rideal, *Interfacial Phenomena*, Academic Press, New York, 1963.
2. T. F. Tadros and B. Vincent, eds., *Encyclopaedia of Emulsion Technology*, Marcel Dekker, 1983.
3. V. N. Paunov, *Langmuir*, 2003, **19**, 7970.

Cite this: DOI: 10.1039/c0xx00000x

www.rsc.org/softmatter

## PAPER

4. A. W. Adamson, *Physical Chemistry of Surfaces*, John Wiley and Sons, New York, 1976.
5. E. M. Furst, *Proceedings of the National Academy of Sciences*, 2011, **108**, 20853-20854.
6. T. S. Horozov, D. A. Braz, P. D. I. Fletcher, B. P. Binks and J. H. Clint, *Langmuir*, 2007, **24**, 1678-1681.
7. E. Dickinson, *Advances in colloid and interface science*, 2011, **165**, 7-13.
8. P. M. Kruglyakov and A. V. Nushtayeva, *Advances in colloid and interface science*, 2004, **108-109**, 151-158.
9. V. N. Paunov, O. J. Cayre, P. F. Noble, S. D. Stoyanov, K. P. Velikov and M. Golding, *J. Colloid Interf. Sci.*, 2007, **312**, 381-389.
10. A. Maestro, L. J. Bonales, H. Ritacco, R. G. Rubio and F. Ortega, *Physical chemistry chemical physics : PCCP*, 2010, **12**, 14115-14120.
11. L. Isa, F. Lucas, R. Wepf and E. Reimhult, *Nature communications*, 2011, **2**, 438.
12. F. Leal-Calderon, S. V. and J. Bibette, *Emulsion Science, Basic Principles* Springer, New York, 2007.
13. B. S. Murray and R. Ettelaie, *Curr. Op. Colloid & Interf. Sci.*, 2004, **9**, 314-320.
14. Z. Du, M. P. Bilbao-Montoya, B. P. Binks, E. Dickinson, R. Ettelaie and B. S. Murray, *Langmuir*, 2007, **19**, 3106-3108.
15. S. Fujii and R. Murakami, *Kona Powder and Particle Journal*, 2008, **26**, 153-166.
16. N. P. Ashby, B. P. Binks and V. N. Paunov, *Chemical Communications*, 2004, 436-437.
17. E. W. Washburn, *Phys. Rev.*, 1921, **17**, 273-283.
18. C. Jouany and P. Chassin, *Colloids Surf.*, 1987, **27**, 289-303.
19. Y. Yuan and T. R. Lee, in *Surface Science Techniques*, Springer, 2013, pp. 3-34.
20. R. N. Wenzel, *Ind. Eng. Chem.*, 1936, **28**, 988-994.
21. O. J. Cayre and V. N. Paunov, *Langmuir*, 2004, **20**, 9594-9599.
22. E. L. Sharp, H. Al-Shehri, T. S. Horozov, S. D. Stoyanov and V. N. Paunov, *RSC Advances*, 2014, **4**, 2201-2213.
23. L. N. Arnaudov, O. J. Cayre, M. A. C. Stuart, S. D. Stoyanov and V. N. Paunov, *Physical Chemistry Chemical Physics*, 2010, **12**, 328-331.
24. K. M. Reed, J. Borovicka, T. S. Horozov, V. N. Paunov, K. L. Thompson, A. Walsh and S. P. Armes, *Langmuir*, 2012, **28**, 7291-7298.
25. S. Ecke, M. Preuss and H. Butt, *J. Adhes. Sci. Technol.*, 1999, **13**, 1181-1191.
26. G. E. Yakubov, O. I. Vinogradova and H.-J. Butt, *J. Adh. Sci. Technol.*, 2000, **14**, 1783-1799.
27. B. P. Binks and S. O. Lumsdon, *Langmuir*, 2000, **16**, 8622-8631.
28. J. C. Berg, *An Introduction to Interfaces & Colloids: The Bridge to Nanoscience*, World Scientific, 2010.
29. V. N. Paunov, B. P. Binks and N. P. Ashby, *Langmuir*, 2002, **18**, 6946-6955.
30. P. A. Kralchevsky, I. B. Ivanov, K. P. Ananthapadmanabhan and A. Lips, *Langmuir*, 2005, **21**, 50-63.